5-7-2021

Cumulative Infiltration and Infiltration Rate Prediction Using Optimized Deep Learning Algorithms: A Study in Western Iran

Mahdi Panahi
Kangwon National University

Khabat Khosravi
Ferdowsi University of Mashhad

Sajjad Ahmad
University of Nevada, Las Vegas, sajjad.ahmad@unlv.edu

Somayeh Panahi
Islamic Azad University, North Tehran Branch

Salim Heddam
Université 20 Août 1955-Skikda

Journal of Hydrology: Regional Studies 35 (2021) 100825

Contents lists available at ScienceDirect

Journal of Hydrology: Regional Studies

journal homepage: www.elsevier.com/locate/ejrh

Cumulative infiltration and infiltration rate prediction using optimized deep learning algorithms: A study in Western Iran

Mahdi Panahi [a,b], Khabat Khosravi [c], Sajjad Ahmad [d], Somayeh Panahi [e], Salim Heddam [f], Assefa M Melesse [g], Ebrahim Omidvar [h], Chang-Wook Lee [a,*]

[a] Division of Science Education, Kangwon National University, College of Education, # 4-301, Gangwondaehak-gil, Chuncheon-si, Gangwon-do, 24341, South Korea
[b] Geoscience Platform Division, Korea Institute of Geoscience and Mineral Resources (KIGAM), 124, Gwahak-ro Yuseong-gu, Daejeon, 34132, South Korea
[c] Department of Watershed Management Engineering, Ferdowsi University of Mashhad, Mashhad, Iran
[d] Department of Civil and Environmental Engineering and Construction, University of Nevada, Las Vegas, USA
[e] Young Researchers and Elites Club, North Tehran Branch, Islamic Azad University, Tehran, Iran
[f] Laboratory of Research in Biodiversity Interaction Ecosystem and Biotechnology, University 20 Août 1955, Route El Hadaik, BP 26, Skikda, Algeria
[g] Department of Earth and Environment, Florida International University, Miami, USA
[h] Department of Watershed Management Engineering, University of Kashan, Kashan, Iran

ARTICLE INFO

Keywords:
Cumulative infiltration
Infiltration rate
Deep learning
CNN
Metaheuristic
Iran

ABSTRACT

Study region: Sixteen different sites from two provinces (Lorestan and Illam) in the western part of Iran were considered for the field data measurement of cumulative infiltration, infiltration rate, and other effective variables that affect infiltration process.

Study focus: Soil infiltration is recognized as a fundamental process of the hydrologic cycle affecting surface runoff, soil erosion, and groundwater recharge. Hence, accurate prediction of the infiltration process is one of the most important tasks in hydrological science. As direct measurement is difficult and costly, and empirical models are inaccurate, the current study proposed a standalone, and optimized deep learning algorithm of a convolutional neural network (CNN) using gray wolf optimization (GWO), a genetic algorithm (GA), and an independent component analysis (ICA) for cumulative infiltration and infiltration rate prediction. First, 154 raw datasets were collected including the time of measuring; sand, clay, and silt percent; bulk density; soil moisture percent; infiltration rate; and cumulative infiltration using field survey. Next, 70 % of the dataset were used for model building and the remaining 30 % was used for model validation. Then, based on the correlation coefficient between input variables and outputs, different input combinations were constructed. Finally, the prediction power of each developed algorithm was evaluated using different visually-based (scatter plot, box plot and Taylor diagram) and quantitatively-based [root mean square error (RMSE), mean absolute error (MAE), the Nash-Sutcliffe efficiency (NSE), and percentage of bias (PBIAS)] metrics.

New Hydrological Insights for the Region: Finding revealed that the time of measurement is more important for cumulative infiltration, while soil characteristics (i.e. silt content) are more significant in infiltration rate prediction. This shows that in the study area, silt parameter, which is

* Corresponding author.
E-mail addresses: mahdi.panahi@kigam.re.kr (M. Panahi), khabat.khosravi@gmail.com (K. Khosravi), sajjad.ahmad@unlv.edu (S. Ahmad), Somayeh.panahi@gmail.com (S. Panahi), heddamsalim@yahoo.fr (S. Heddam), melessea@fiu.edu (A.M. Melesse), ebrahimomidvar@gmail.com (E. Omidvar), cwlee@kangwon.ac.kr (C.-W. Lee).

https://doi.org/10.1016/j.ejrh.2021.100825
Received 27 September 2020; Received in revised form 20 April 2021; Accepted 24 April 2021
Available online 7 May 2021

the dominant constituent parameter, can control infiltration process more effectively. Effectiveness of the variables in the present study, in the order of importance are time, silt, clay, moisture content, sand, and bulk density. This can be related to the fact that most of study area is rangeland and thus, overgrazing leads to compaction of the silt soil that can lead to a slow infiltration process. Soil moisture content and bulk density are not highly effective in our study because these two factors do not significantly change across the study area. Findings demonstrated that the optimum input variable combination, is the one in which all input variables are considered. The results illustrated that CNN algorithms have a very high performance, while a metaheuristic algorithm enhanced the performance of a standalone CNN algorithm (from 7% to 28 %). The results also showed that a CNN-GWO algorithm outperformed the other algorithms, followed by CNN-ICA, CNN-GA, and CNN for both cumulative infiltration and infiltration rate prediction. All developed algorithms underestimated cumulative infiltration, while overestimating infiltration rates.

1. Introduction

The soil-water infiltration process plays a fundamental role in hydrology, pedology, hydrogeology, irrigation, and drainage systems (Kale and Sahoo, 2011; Mahapatra et al., 2020; Ghumman et al., 2018a). From a computational point of view, the infiltration can be defined as the ability of water to move into the soil strata (Angelaki et al., 2013). Total amount of water that soil strata are able to absorb from rainfall or irrigation in a given time is considered as a cumulative infiltration (*F(t)*); the velocity of the water entering into the soil in a given period of time is defined as the infiltration rate; (*f(t)*) and the velocity of water entering into the soil in a specific amount of time is defined as an instantaneous infiltration rate (Hooshyar and Wang, 2016; Mahmood and Latif, 2003). The rate of water infiltration into soil is controlled by several factors such as the initial moisture conditions of the ground's surface; rainfall intensity; soil and water temperature; biological activities in the soil column; soil texture, porosity, and compactness; and surface cover conditions (Angelaki et al., 2013; Ma et al., 2015; Hooshyar and Wang, 2016).

Infiltration contributes to groundwater recharge; the movement of soil solutes through the ground; the water budget of vegetation; runoff/flood generation; and soil erosion. In addition, the movement of chemical contaminants through soil and into groundwater is mainly controlled by the water infiltration process and overall watershed management plans (Angelaki et al., 2004; Mahapatra et al., 2020). In addition, the success of surface irrigation methods is mainly governed by soil infiltration characteristics (Ghumman et al., 2018b; Fan et al., 2018), and the efficiency of irrigation depends largely on the spatial and temporal variations in the infiltration characteristics (Khatri and Smith, 2006). Therefore, quantifying the infiltration process is important in watershed management.

Over the years, several authors worldwide have highlighted the difficulties encountered in direct soil water infiltration measurement, which is a labor intensive and time consuming task (Huang et al., 2016; Jejurkar and Rajurkar, 2015; Stephen et al., 2010; Puri et al., 2011). Therefore, various physical and empirical equations have been developed for infiltration prediction based on the knowledge of water movement in the soil, according to soil hydraulic properties (Lassabatere et al., 2009). Some example of these equations are Green and Ampt (1911); Philip (1957a), b; Richards (1931), the United States Department of Agriculture (USDA) Soil Conservation Service SCS (1972), Horton (1941), and Kostiakov (1932). Some drawbacks of these algorithms, except simplicity, which make them incapable to predict *F(t)* are homogeneity of soil and constant soil moisture content (Singh et al., 2019a). Additionally, these models involve only one or a few of the input variables, while some effective variables such as soil texture and degree of compactness are neglected. Although numerical and physically based models (i.e., TOPMODEL and HYDRUS-3D) can predict the infiltration process accurately, the acquisition of data with high spatial resolutions (i.e., heterogeneous soil data), which is required for running these models, is a difficult task, especially for large catchments. Moreover, recently, infiltration processes have changed to a certain extent, due to soil macro-pores (Demand et al., 2019) and soil biological activities (Cheik et al., 2018; Zaller et al., 2014; Fan et al., 2020a, b)).

Recently, there have been increased efforts to propose alternative methods for accurately estimating the amount of soil water infiltration, using different kinds of models based on data driven/machine learning models (Angelaki et al., 2018; Rahmati, 2017; Sihag et al., 2018a, a; Sihag et al., 2020b, b; Sepahvand et al., 2018). Some benefits of these types of algorithms can be summarized as: strong prediction performance; easy and fast to develop; robustness to missing data; and the ability to handle large amounts of data at different scales (Ahmad and Simonovic, 2005; Ahmad et al., 2010; Choubin et al., 2014; Kisi et al., 2012; Yaseen et al., 2015; Ateeq-ur-Rauf et al., 2018; Thakur et al., 2020).

Rahmati (2017) compared the group method of data handling (GMDH), multilayer perceptron artificial neural network (MLPNN), and multiple linear regression (MLR) models, in predicting cumulative infiltrations (*F(t)*), using soils' readily available characteristics (RAC_s): (*i*) soil primary particles (clay, silt, and sand), (*ii*) saturated hydraulic conductivity (K_s), (*iii*) soil densities (bulk and particle), (*iv*) organic carbon, (*v*) wet-aggregate stability, (*vi*) electrical conductivity, and (*vii*) soil antecedent (θ_i) and field saturated (θ_{fs}). The study was conducted in Iran, and the obtained results showing that: (*i*) among the RAC_s characteristics, the K_s has the most influence on the model's accuracy; and (*ii*) the best accuracy was obtained using the GMDH models.

Singh et al. (2017) compared random forest regression (RF), MLPNN, and M5Tree models in predicting soil's infiltration rate, and showed that the RF model was more accurate. The authors compared the genetic programming (GP), support vector machine (SVM), multiple linear regression (MLR) models, with Kostiakov and Philip's models in predicting the cumulative infiltration of sandy soil. According to the obtained results, the GP model was superior, followed by the SVM model, the MLR model, and the Kostiakov model.

Table 1
Past and present studies of infiltration characteristics prediction.

No.	Authors	algorithms	Target variable	Efficient algorithms
1	Sy, 2006	ANN, Philip and Green-Ampt models	Cumulative Infiltration (laboratory)	ANN
2	Anari et al., 2011	ANN, ANFIS, Local Linear Regression (LLR), and Dynamic Local Linear Regression (DLLR)	Infiltration rate (field)	ANN
3	Das et al., 2012	ANN and SVM	Hydraulic conductivity (field)	SVM
4	Yilmaz et al., 2012	ANN and ANFIS	Permeability of soil (laboratory)	ANFIS
5	Rahmati, 2017	GMDH, MLR, and ANN	Pedo-transfer functions (field)	GMDH
6	Singh et al., 2017	RF, ANN, and M5P	Infiltration rate (laboratory)	RF
7	Sihag et al., 2017	SVR, GP, and MLR	Cumulative infiltration (laboratory)	GP
8	Sihag et al., 2020c	SVR, MLR, M5P, and GRNN	cumulative infiltration (laboratory)	SVR
9	Sihag et al., 2020b	ANN, GP, GRNN, and GEP	Infiltration rate (field)	ANN
10	Sihag et al., 2019c	ANFIS, ANN, and MLR	Unsaturated hydraulic conductivity (laboratory)	MLR
11	Sihag et al., 2019a	M5P, Bagging-M5P, RF, and Bagging-RF	Cumulative infiltration (laboratory)	Bagging-M5P
12	Singh et al., 2019b	SVM, GP, RF, and MLR	permeability of the soil (laboratory)	SVM
13	Sihag et al., 2019d	RF, M5P, and MLR	unsaturated hydraulic conductivity (field)	RF
14	Singh et al., 2019a	SVM, GP, M5P, and MLR	infiltration rate(laboratory)	M5P
15	Sihag et al., 2019d	ANFIS, ANFIS-FFA, and ANFIS-PSO	unsaturated hydraulic conductivity (field)	ANFIS-FFA and ANFIS-PSO
16	Kumar and Sihag, 2019	RF and ANFIS	Infiltration rate(field)	RF
17	Sihag et al., 2020a	SVM, GP, ANN, RF, Philip's model and Kostiakov model	infiltration rate (laboratory)	GP
18	Sihag et al., 2020c	SVR-RBF, SVR-Poly, MLR, M5P, GRNN	cumulative infiltration (laboratory)	SVR-RBF

Angelaki et al. (2018) applied several machine learning models, namely, an adaptive neuro-fuzzy inference system (ANFIS), SVM, and MLPNN models, in predicting cumulative infiltration. The best accuracy was obtained using the ANFIS model with a triangular membership function, followed by the MLPNN, and the SVM models.

Sihag et al. (2018a), b; Sihag et al. (2019b), and Sepahvand et al. (2018) compared ANN, Gene Expression Programming (GEP), ANFIS, SVM and RF algorithms for cumulative infiltration prediction, and stated that the ANFIS model had the highest performance followed by the SVM, RF, ANN, and GEP algorithms. Sihag et al. (2020a) compared the ANN, SVM, RF, GP machines learning models with Kostiakov's and Philip's models, in predicting infiltration rate using various input variables. They reported that the best accuracy was obtained using the GP with polynomial function, while the lowest accuracy was obtained using the Philip's model. Sihag et al. (2020b) used the SVM with a radial basis function neural network (SVM-RBF), SVM with a polynomial (SVM-PO) kernel function, GRNN, M5Tree, and MLR models in predicting cumulative infiltration. The best accuracy was achieved using SVM-RBF, while the lowest accuracy was achieved using the GRNN model. Pahlavan-Rad et al. (2020) applied MLR and RF for spatial prediction of soil water infiltration in south-eastern Iran. They concluded that although both algorithms have a reasonable prediction power, RF algorithm outperforms MLR. Resulting from a through literature review, a summary of the developed algorithms for infiltration process prediction is presented in Table 1.

According to the literature review, there is not a global algorithm that is perfect in all cases; thus, new robust algorithms are highly recommended. The ANN algorithm is one of the oldest developed algorithms but this algorithm has various drawbacks such as slow convergence speed (Kisi et al., 2012; Melesse et al., 2011). SVM can be time consuming to train since it is very sensitive to hyper-parameter selection (Ahmad et al., 2018). RF, as a robust algorithm, suffers from its complexity as well as being time-consuming to build. GMDH, SVM, ANN, SVM, and other similar algorithms suffer from accurate determination of the models' parameters, especially weights in membership functions, while their integration with metaheuristic algorithms has improved their prediction power significantly (Bui et al. 2018).

Another limitation of these algorithms is that they only have one hidden layer in their structure. Lately, deep learning algorithms [i.e., Convolution Neural Networks (CNN)] which benefit from various hidden layers, have been developed for solving more complex process with a higher degree of accuracy. CNN algorithms are one of the well-known types of DL, which were developed for non-time series datasets (spatial distribution). This kind of DL algorithm has been successfully applied for natural hazard susceptibility mapping, including flash floods (Bui et al., 2020a) and landslides (Bui et al., 2020b; Wang et al., 2020), while they have not been used for hydrologic forecasting problems yet. Additionally, these robust, strong, and high level algorithms have many parameters in their structures that need to be optimized, similar to ANN, ANFIS, and so on.

In the present research, the prediction capability of a standalone CNN model and a CNN optimized algorithm, using a genetic algorithm (CNN-GA), grey wolf optimization (CNN-GWO), and an imperialist competitive algorithm (CNN-ICA) were investigated for cumulative infiltration and infiltration rate prediction using in-situ observations of sand (%), clay (%), silt (%), density (g/cm^3), and moisture content (%) as input variables. The main idea was to evaluate the robustness of the new hybrid models using different input variables. To the best of the authors' knowledge, this is the first time that a deep learning algorithm was optimized using metaheuristic algorithms in the field of Geoscience. Even a standalone CNN algorithm has not been used for hydrologic prediction/ forecasting so far.

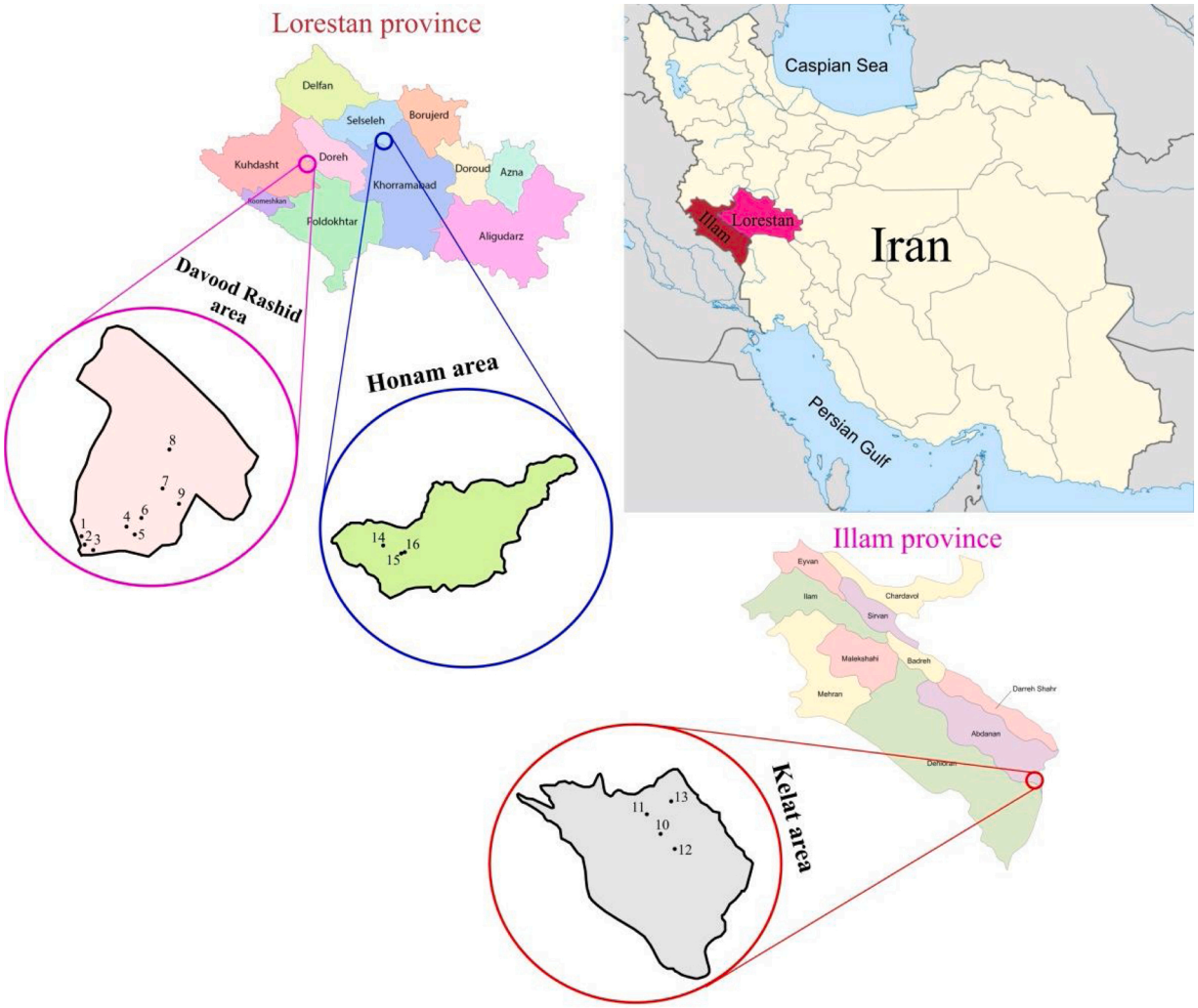

Fig. 1. Study area and location of 16 sites for the experiment.

Table 2
Coordinates of the 16 sites (Sepahvand et al., 2018).

No	Province	Longitude	Latitude
1	Illam	47°50′45.86″E	32°38′33.64″N
2	Illam	47°50′42.02″E	32°38′37.16″N
3	Illam	47°50′49.64″E	32°38′30.64″N
4	Illam	47°50′48.39″E	32°38′39.88″N
5	Lorestan	47°41′33.06″E	33°33′54.13″N
6	Lorestan	47°41′40.52″E	33°33′49.14″N
7	Lorestan	47°41′45.94″E	33°33′58.93″N
8	Lorestan	47°42′6.56″E	33°34′17.67″N
9	Lorestan	47°42′20.06″E	33°34′8.07″N
10	Lorestan	47°42′12.19″E	33°34′41.89″N
11	Lorestan	47°40′50.51″E	33°33′48.08″N
12	Lorestan	47°40′54.40″E	33°33′43.24″N
13	Lorestan	47°41′1.05″E	33°33′40.29″N
14	Lorestan	48°15′55.80″E	33°47′25.37″N
15	Lorestan	48°17′15.25″E	33°47′4.12″N
16	Lorestan	48°17′23.76″E	33°47′6.80″N

Table 3
Descriptive statistics of the training and testing datasets.

Variables	Training Dataset				Testing Dataset			
	Min	Max	Mean	Std. Deviation	Min	Max	Mean	Std. Deviation
Time [T] (min)	2.5	70	23.99	17.36	2.5	60	23.33	15.48
Sand [S_a] (%)	6	38	25.73	9.21	6	38	24.96	9.26
Clay [C] (%)	10	52	23.76	13.12	10	52	24.24	13.29
Silt [S_i] (%)	37	65	50.39	7.55	37	65	50.67	7.71
Density [D] (g/cm^3)	1.08	1.79	1.42	0.17	1.08	1.79	1.41	0.16
Moisture [M_C] (%)	1.66	3.84	2.42	0.53	1.66	3.84	2.42	0.54
Infiltration rate [$f(t)$] (cm/h)	0.08	1.56	0.28	0.23	0.08	1.52	0.28	0.24
Cumulative infiltration [F(t)] (cm)	0.3	27.1	6.93	5.56	0.6	25.2	7.00	5.49

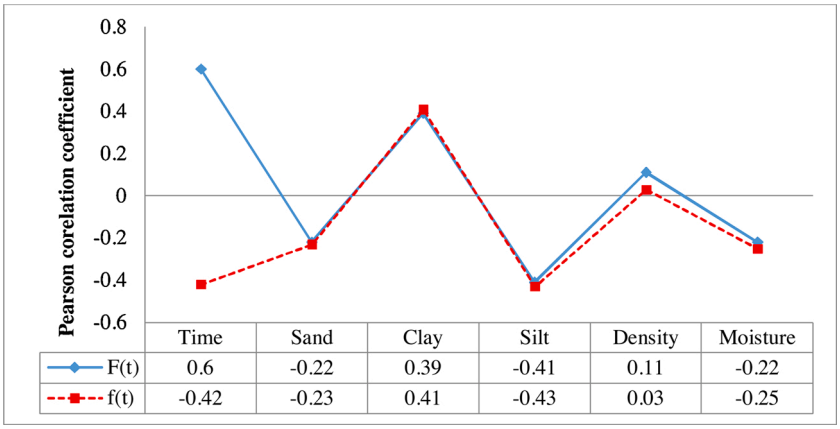

Fig. 2. Determination of input variables' importance using the Pearson correlation coefficient.

2. Study area

Sixteen different sites from two provinces (Lorestan and Illam) in the western part of Iran were considered for the field data measurement of cumulative infiltration, infiltration rate, and other effective variables. Nine sites from the Davood Rashid region, three sites from the Honam areas, and four sites from the Kelat region in the Illam provinces were selected (Fig. 1 and Table 2). The maximum and minimum elevation of the study area is about 3300 and 2100 m, respectively (Behrahi et al., 2018). The study areas have a humid climate with mean annual rainfall of 550 mm. Rangeland covers most of the study areas, while forest land, dry farming, and irrigation-land are considerable. More information about study areas is provided in Sihag et al. (2019c) and Sepahvand et al. (2018).

3. Methodology

3.1. Field measurement and data collection

One hundred and fifty-four raw datasets, including cumulative infiltration (F(t)), infiltration rate (f(t)), % of sand (S_a), % of silt (S_i), % of clay (C), soil bulk density (D), and moisture content (M_C), were measured and compiled from 16 sites by Sepahvand et al. (2018). The field measurements were carried out using a double-ring infiltrometer, with a depth of 30 cm, and inner and outer diameters of 30 cm and 60 cm, respectively. At first, both rings were driven about 10 cm with a sledgehammer. Next, both inner and out rings were filled by water at a given depth. Measurements were carried out in the inner ring while the outer ring water was used to prevent leaching from the inner ring, which is one of the sources of error. Measurements were taken at time intervals of 2.5, 5, 15, 20, 30, 35, 40, 50, and 70 min, and continued until the infiltration rate became steady.

The compiled dataset was divided into two subsets randomly; 70 % (107 raw data points) of the data were used for model constructing, while the remaining 30 % (47 raw data points) were employed for model evaluation. There is no universal guideline for data splitting, but a 70:30 ratio is the most widely used method in both time series and spatial prediction (Samadianfard et al., 2018, 2019; Pham et al., 2017)). Descriptive statistics of the training and testing datasets are tabulated in Table 3.

Table 4
Different input combinations applied in the current study.

No.	Different input combination for F(t)	Different input combination for f(t)
1	T	Si
2	T, Si	Si, T
3	T, Si, C	Si, T, C
4	T, Si, C, Sa	Si, T, C, M
5	T, Si, C, Sa, M	Si, T, C, M, Sa
6	T, Si, C, Sa, M, D	Si, T, C, M, Sa, D

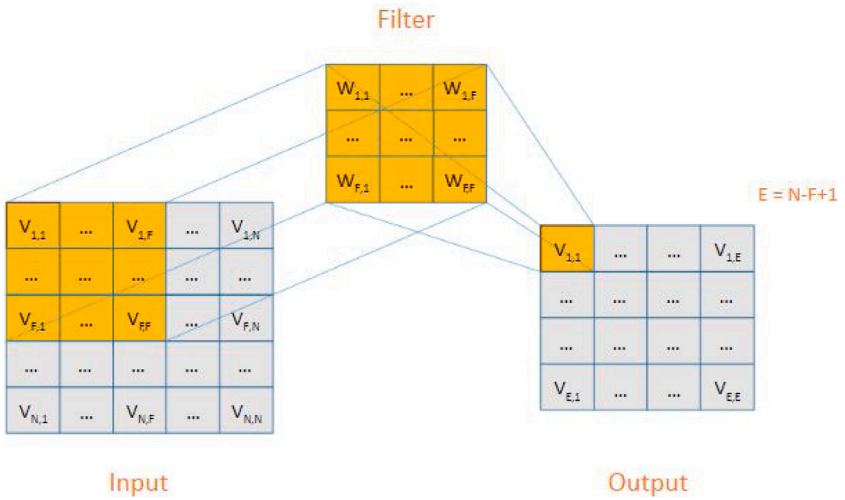

Fig. 3. Applying filter (F × F) to the input data (N × N) in order to get value of V1,1 in the next layer (Hoseinzade and Haratizadeh, 2019).

3.2. Input combination construction

Each variable has a different impact on the infiltration process; hence, the correct selection of input variables has an influential effect on the predictive capability of the developed algorithms, while irrelevant data reduce models' performance. Correlation coefficient (r) criteria between input variables and outputs (Fig. 2) was utilized as a foundation metric to construct different input combinations (Table 4).

At the first stage, the variable with the highest correlation coefficient (T for F(t) and Si for f(t)) was considered as a single input variable to the model. The assumption here is to determine whether the variable with highest impact has the ability to predict the infiltration process individually. Next, the second combination was constructed by adding variables with the second highest r to the first combination, and this approach was continued until variables with the lowest r were added to the combinations to build the last input combination. Each developed algorithm was performed with all input combinations, and finally, based on the Root Mean Square Error (RMSE); the best input combination for each model was determined and used for further analysis.

3.3. Determination of optimal values for each operator

As there is no an optimum global value for model operators that works perfectly for all the cases, model parameter optimization is one of the most important, as well as the last step among the modeling process. In the present study, different meta-heuristic algorithms were applied to find the optimum values, especially weights in the membership function of the deep CNN algorithm. GA, GWO, and ICA can be applied to train a CNN, with the main intention of achieving the exact required accuracy, and minimizing the network complexity indicators, as well as the approximation error accuracy. In order to fulfill this purpose, computing the standard error on the training set and the fitness function of the vector solution can be done. In this study, the fitness function (f) is determined as

$$f = 0.5\left(\sqrt{\frac{\sum_{i=1}^{n}(o-y)^2}{R}}\right) \quad (1)$$

where o represents the desired output, y stands for the actual output, and R shows the number of training data. This process can be stopped when the fixed predefined iteration is done, and the calculating fitness function is less than a specified constant. In this condition, the approximate error accuracy is minimum, and the network complexity indicators have their optimum amount.

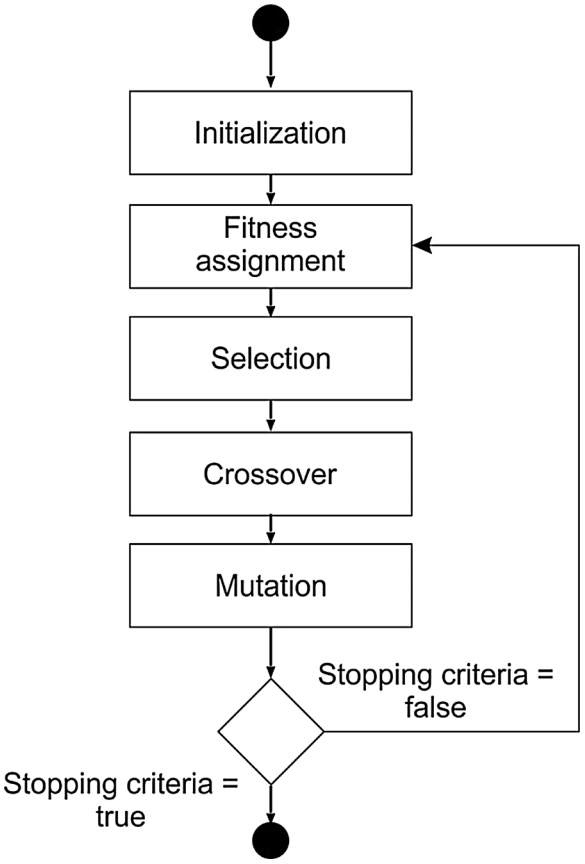

Fig. 4. GA general flowchart.

3.4. Models background theory

Scientists have designed numerous Deep Learning (DL) algorithms (Goodfellow et al., 2016) for performing optimization in various domains such as object detection and object recognition (Wu et al., 2019). DL builds complex concepts by combining simpler concepts (Goodfellow et al., 2016). All algorithms were implemented using MATLAB programming software.

3.4.1. Convolutional neural network (CNN)

A Convolutional Neural Network (CNN) is a type of multi-layer and feed forward neural network (Di Persio and Honchar, 2016; Gunduz et al., 2017). The concept of CNN was introduced by Fukushima (1988) without wide application (Fukushima, 1988), and LeCun and Bengio (1995) presented a CNN in 1995 with successful results in the classification of digital handwriting. This technique is a multi-layer algorithm and consists of three main types of layers, including a convolutional layer, pooling layer, and fully connected layer. The first layer is used to measure changes by a pre-defined filter (F × F) on the input layer (N × N) matrix. To put it another way, Eq.2 calculates input of layer l in order to obtain the value of $v_{i,j}^{l}$ in the next layer in Fig. 3 (Hoseinzade and Haratizadeh, 2019).

$$v_{i,j}^{l} = \delta\left(\sum_{k=0}^{F-1}\sum_{m=0}^{F-1} w_{k,m} V_{i+k,j+m}^{l-1}\right) \tag{2}$$

The pooling layer has the main responsibility to reduce the spatial size. Therefore, this layer can control the risk of the over fitting problem in CNNs. Finally, the fully connected layer converts the extracted features between two layers of the CNN, the previous layer to the final output layer, by the following equation:

$$v_{i}^{j} = \delta\left(\sum_{k} v_{k}^{j-1} w_{k,i}^{j-1}\right) \tag{3}$$

Detailed information about CNNs can be found in (Ding, 2020; Indolia et al., 2018; Kujawa et al., 2020; Zhu et al., 2019).

3.4.2. Genetic algorithm (GA)

The original Genetic Algorithm (GA) was investigated by John Holland in 1975 (Kofinas et al., 2018). This algorithm is designed as

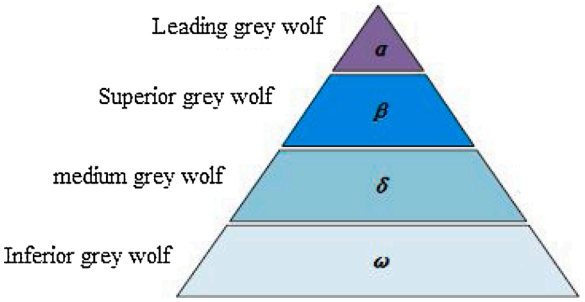

Fig. 5. The social hierarchy of grey wolves (Mirjalili et al., 2014).

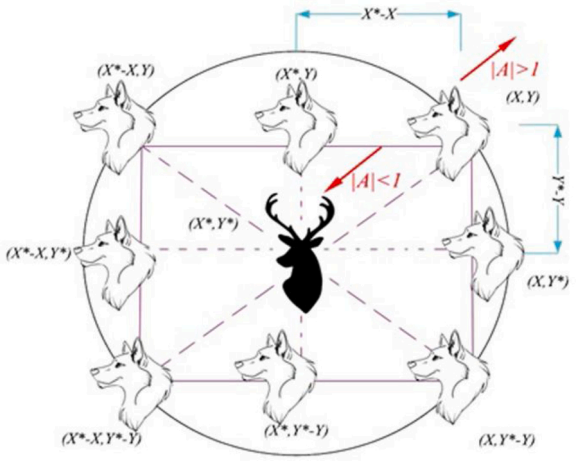

Fig. 6. Position updating mechanism of search agents, and effects of A on it (Mirjalili et al., 2014).

optimization tool to provide an optimal solution for variety applications in science and engineering (Kakandikar and Nandedkar, 2016). GA is a class of population-based algorithms, with two fundamental operators, crossover and mutation, in Fig. 4 (Rozinajová et al., 2018).

In this method, the incipient generation selects randomly. Afterward, both operators generate new member of the population for the next generation (Maiti and Maiti, 2008; Sivanandam and Deepa, 2008). A crossover operator is used to combine the genetic information (two chromosomes) to create new member (new chromosomes) (Rozinajová et al., 2018). The aim of the mutation operator is to impede from being captured in the local optimal solution (Yang et al., 2014). This operator protects the genetic diversity of a new generation of chromosomes to the next (Montazeri-Gh et al., 2006). The numerous mutation genes of the new population are called (n_g), which is the multiplication mutation rate (M_r) and the length of genes (l_g), as follows (Iyer et al., 2019):

$$n_g = l_g \times M_r \tag{4}$$

3.4.3. Grey wolf optimizer (GWO)

Grey Wolf Optimizer (GWO) is one of the popular algorithms based on the diverse natural occurrences of the hunting behavior grey wolves (Mirjalili et al., 2014). GWO belongs to the class of meta-heuristic algorithms introduced by Mirjalili in 2014.

The structure of the grey wolf is similar to a pyramid of four levels, as it consists of alpha (α), beta (β), delta (δ), and omega (ω) wolves from top to bottom, as shown Fig. 5 (Hu et al., 2020). As the pyramid clearly shows, alpha wolves are the top and the optimal solutions that are the leaders of the wolves for making decisions (Dehghani et al., 2019). This pyramid illustrates that the second level and third level are called beta and delta, respectively, and are subservient wolves in decision-making or other pack processes (Luo and Zhao, 2019), as well as suboptimal solutions (Li et al., 2020). Finally, omegas play the role of the scapegoat wolves (Dehghani et al., 2019) and the rest of the solutions (Li et al., 2020). The process of hunting of GWO consists of four steps.

Firstly, as shown in Fig. 6, the wolves encircle prey during a hunt (Karasu and Saraç, 2020). Afterwards, grey wolves get closer to the prey and harass it. GWO achieves the best solution to update the positions of other wolves according to the positions of α, β, and δ wolves. The hunting process finishes, and the wolves attack towards the prey. It depends on the values of A and C, which are determined by the following formula:

$$\overrightarrow{C} = 2a.\overrightarrow{r}_1 \tag{5}$$

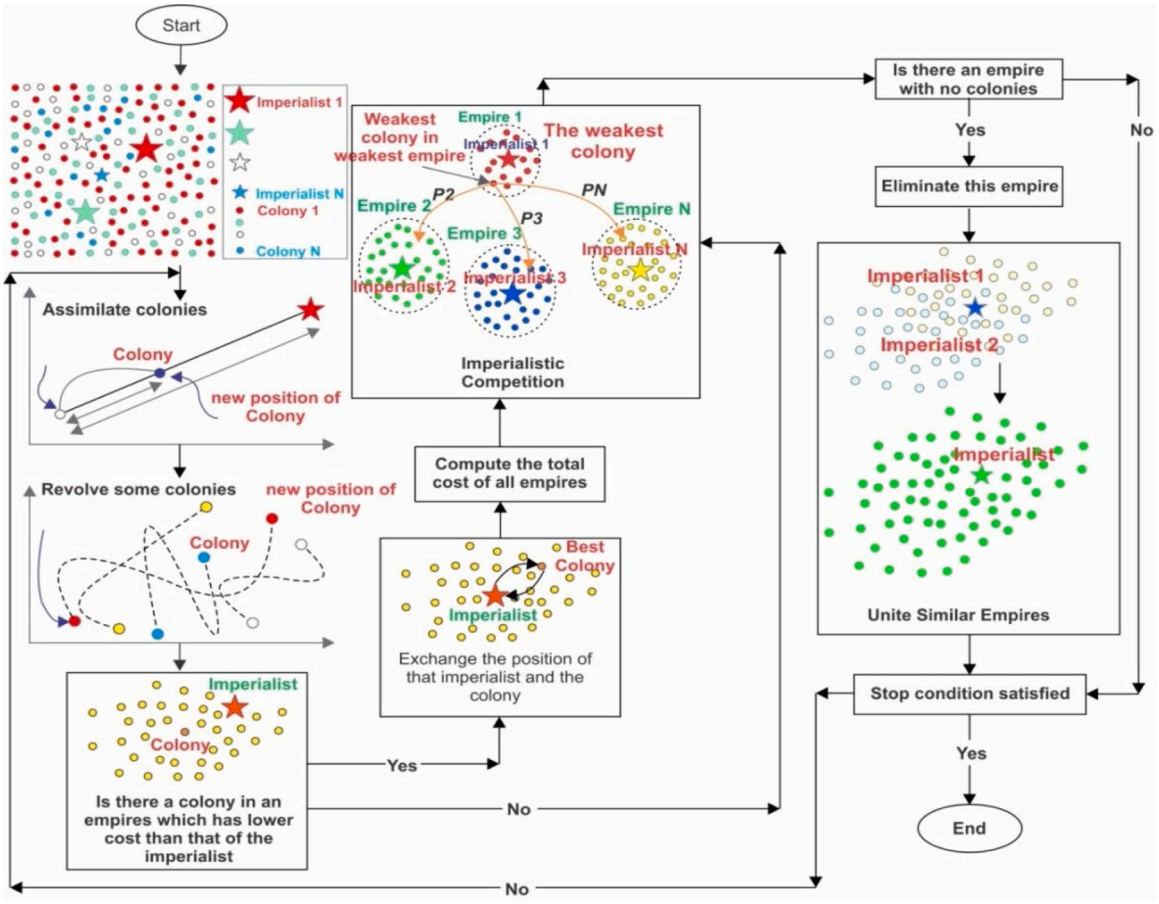

Fig. 7. Flowchart of Independent Component Analysis (Atashpaz-Gargari and Lucas, 2007).

$$\overrightarrow{A} = 2a.\overrightarrow{r}_2 - a \tag{6}$$

where $\overrightarrow{r}_1$ and $\overrightarrow{r}_2$ are random numbers between 0 and 1 used to calculate the coefficient vectors of $\overrightarrow{A}$ and $\overrightarrow{C}$, and a is a vector that decreases linearly from 2 to 0 (Saxena et al., 2020).

Theses coefficients' vectors can be two states during the process of GWO. The first state is $|A| < 1$ and $|C| < 1$, which means that the wolves tend to attack the prey (Yang et al., 2017). In contrast, the second state occurs by the range of $|A| > 1$ or $|A| < -1$ and $|C| > 1$, which means that the wolves will leave the current position prey and find another potential prey (Yang et al., 2017). This step is called searching for prey or the exploration step (Rashid et al., 2019).

3.4.4. *Imperialist competitive algorithm (ICA)*

One of the evolutionary algorithms is achieved by the human socio-political process that is called Imperialistic Competition Algorithm (ICA) (Reisi et al., 2019) by using the mathematical model and computer simulation (Barkhoda and Sheikhi, 2020). ICA is proposed by Atashpaz and Lucas to solve various optimization problems by high and speed convergence rate (Atashpaz-Gargari and Lucas, 2007) according to the flowchart in Fig. 1 (Roshanaei et al., 2009) (Fig. 7).

ICA is such as other evolutionary algorithms by random initial population that every one of them is named a country (Barkhoda and Sheikhi, 2020). The third steps of ICA are presented according to countries as follows (Dehghani et al., 2021):

1. Initialization empires

The parameter of countries is p_d^i, each of them is determined based on the problem that it means i th country in the d th dimension in Eq. (7). The number of primary countries is shown by N_c in Eq. (8).

$$country_i = \left[p_1^i, \ldots, p_d^i, \ldots, p_{N_{var}}^i\right] \tag{7}$$

$$c_i = f(country_i) = f\left(p_1^i, \ldots, p_d^i, \ldots, P_{N_{var}}^i\right),\ i = 1, \ldots, N_c \tag{8}$$

The power of a country indicates whether it is an imperial or a colony. Details of the colonies associated with each empire can be found here (Roshanaei et al., 2009).

2. Assimilation colonies and revolution

Each imperialist conquers a number of colonies and forms a powerful empire, and then the imperialist rivalry between empires begins. If an empire fails to rise or loss its power, it will disappear during imperialist competition. So the secret of the survival of an empire depends on its ability and effort to conquer the colonies from enemy empires (Barkhoda and Sheikhi, 2020) then they move toward the imperialist by x units (Dehghani et al., 2021). The new location of colony is in Eq. (9).

$$x \sim U(0, \beta \times d), \beta > 1 \tag{9}$$

U, β and d in Eq. (c) are a random number between 0 and 1, a number larger than one and distance between colony and its imperialist location, respectively. The colony and its imperialist move in different location when colony finds the best location, after that situation of colony and its imperialist are changed until only one powerful empire exists (Dehghani et al., 2021).

3.5. Model validation

Four different quantitative and visual metrics are applied for model performance validation and comparison. Visual comparison including a line graph, scatter plot, box plot, and Taylor diagram, except for fast, desirable, and interesting methods, benefit from detailed information about maximum and minimum accurate prediction (line graph and box plot), as well as mean, first, and third quartile accurate prediction (box plot), which are quantitative metrics weak to report. A Taylor diagram benefits from involving three matrices of RMSE, r, and standard deviation instantaneously (Sigaroodi et al., 2014).

As performance classification, and ranking/ordering of the developed algorithms cannot be determined using visual criteria; hence, four different quantitative criteria, including RMSE, mean absolute error (MAE), the Nash-Sutcliffe efficiency (NSE), and percentage of bias (PBIAS) were calculated as follows (Moriasi et al., 2007; Krause et al., 2005):

$$RMSE = \sqrt{\frac{1}{N}\sum_{i=1}^{N}[M-P]}, \ 0 \le \text{RMSE} < \infty \tag{10}$$

$$MAE = \frac{1}{N}\sum_{i=1}^{N}|M-P|, \ 0 \le \text{MAE} < \infty \tag{11}$$

$$NSE = 1 - \frac{\sum_{i=1}^{N}[M-P]^2}{\sum_{i=1}^{N}\left[M-\overline{M}\right]^2}, \ -\infty < \text{NSE} < 1 \tag{12}$$

$$PBIAS = \frac{\sum_{i=1}^{N}[M-P]}{\sum_{I=1}^{N}M} * 100, \ -\infty \le \text{PBIAS} \le \infty \tag{13}$$

$$R^2 = \left(\frac{\sum_{i=1}^{n}(M-\overline{M})(P-\overline{P})}{\sqrt{\sum_{i=1}^{n}\left(M-\overline{M}\right)^2}\sqrt{\sum_{i=1}^{n}\left(P-\overline{P}\right)^2}}\right)^2 \tag{14}$$

where M and P are the measured and predicted values, respectively; and $\overline{M}$ and $\overline{P}$ arethe mean measured and predicted values.

RMSE and MAE have the same error unit as the target value and this makes it easier to interpret results. NSE is a dimensionless criterion and makes it possible for a comprehensive comparison. PBIAS determines how well the applied model predicts the average magnitudes of the target variable. Performance classification of different criteria is as follows:

1-The lower the RMSE and MAE, the higher the prediction performance.

2- Based on the NSE, classification performances are $0.75 < \text{NSE} \le 1.00$ (very good), $0.65 < \text{NSE} \le 0.75$ (good), $0.50 < \text{NSE} \le 0.65$ (satisfactory), $0.40 < \text{NSE} \le 0.50$ (acceptable), and $\text{NSE} \le 0.4$ (unsatisfactory) (Ayele et al., 2017).

3- Based on the PBIAS classification performances are, $\text{PBIAS} < \pm 10$ (very good), $\pm 10 \le \text{PBIAS} < \pm 15$ (good), $\pm 15 \le \text{PBIAS} < \pm 25$ (satisfactory), $\text{PBIAS} > \pm 25$ (unsatisfactory) (Legates and McCabe, 1999). PBIAS can be used to determine the over-prediction or under-prediction of the developed algorithms (Moriasi et al., 2007).

4- As suggested by Moriasi et al. (2007), R^2 values of $0.7 < R^2 < 1$, $0.6 < R^2 < 0.7$, $0.5 < R^2 < 0.6$, and $R^2 < 0.5$ were considered as very good, good, satisfactory, and unsatisfactory, respectively.

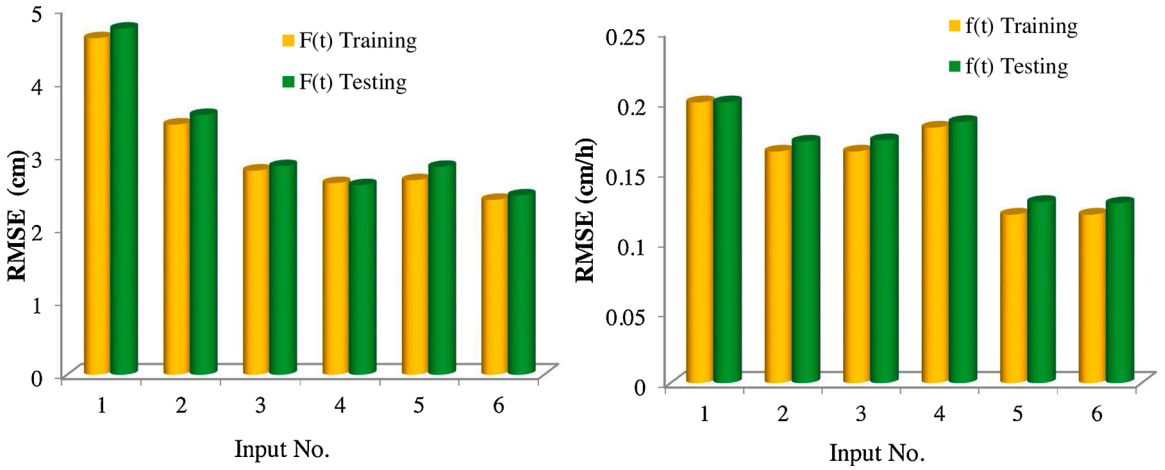

Fig. 8. Identification of the best input combination for F (t) and f (t) prediction using RMSE.

4. Results and discussion

4.1. Input variables importance

As mentioned in Section 3.1, different input variables of time of measurement; sand, silt, and clay content; soil bulk density; and moisture content were considered, based on the data availability and theory of infiltration in order to predict the cumulative infiltration and infiltration rate. Results demonstrated that the time of measuring and silt content are the most effective variables on F(t) and f(t), respectively (Fig. 2), while soil density has the lowest effect on both F(t) and f(t). This reveals that soil texture and its content have a greater effect on the infiltration process than soil density and its compactness. One reason that shows soil moisture content and bulk density has the lowest effect in our study area is that, these two factors do not change significantly across the study areas. These results are in accordance with Singh et al. (2017 and 2020), which stated that time is the most important input variable on cumulative infiltration. Zolfaghari et al. (2012) stated that soil texture properties have a great effect on cumulative infiltration. Variables' effectiveness on F(t) and f(t) are not always constant, and depend on many factors like catchment characteristics, landuse/cover, physical and chemical soil characteristics, and so on (Sy. 2006). Singh et al. (2017) simulated the effect of water quality on infiltration rate and showed that among the input variables of cumulative time, type of impurities, concentration of impurities, and moisture content, cumulative time is the most effective variable on the infiltration rate of the soil.

Results illustrated that time is one of the most efficient variables on both F(t) ($r = 0.60$) and f(t) ($r = -0.42$) According to the r, time has a direct relationship with cumulative infiltration and shows that the more the time, the larger the cumulative infiltration. On the other hand, infiltration rate has an inverse relationship with time showing infiltration rate decreases with time. Additionally, with the passing of time, the f(t) trend is descending, until it reaches a constant rate, which is called the constant or equilibrium infiltration rate, or constant final infiltration capacity.

4.2. Best input combination

The six input variables mentioned earlier were used to construct different input combinations based on RMSE for F(t) and f(t) prediction, respectively. The input combination with the lowest RMSE values were considered be the most effective input combination in improving the prediction capability of F(t) and f(t) (Table 2 and Fig. 8).

For the F(t) prediction, the model with the input combination No. 6, which included all variables (i.e., T, Si, C, Sa, M_c, and D) had the best performance in the training (RMSE = 2.39 cm) and testing (RMSE = 2.45 cm) phases. For f(t) prediction, the model with the input combination No. 6, which again included all input variables (i.e., T, Si, C, Sa, M_c, and D) had the highest performance in the training (RMSE = 0.120 cm) and testing (RMSE = 0.128 cm) steps. According to Fig. 8, by increasing the input variables for both F(t) and f(t), the model's prediction power increases. Singh et al. (2019a) found that the variable combination including time, sand, clay, silt, density, and moisture content was the most effective combination for F(t) and f(t) modeling using SVM and RF models. This is due to this fact that infiltration has a complex process, and using fewer variables, reduces the accuracy of its prediction; therefore, using more relevant and effective variables containing relevant information, important to the infiltration process, enhanced the model's performance.

4.3. Model evaluation

As a training dataset is used for the identification of optimal input variable combinations for F(t) and f(t) prediction, and then model development, the training data cannot be used in the model validation step. Results of this phase only indicate how well the built

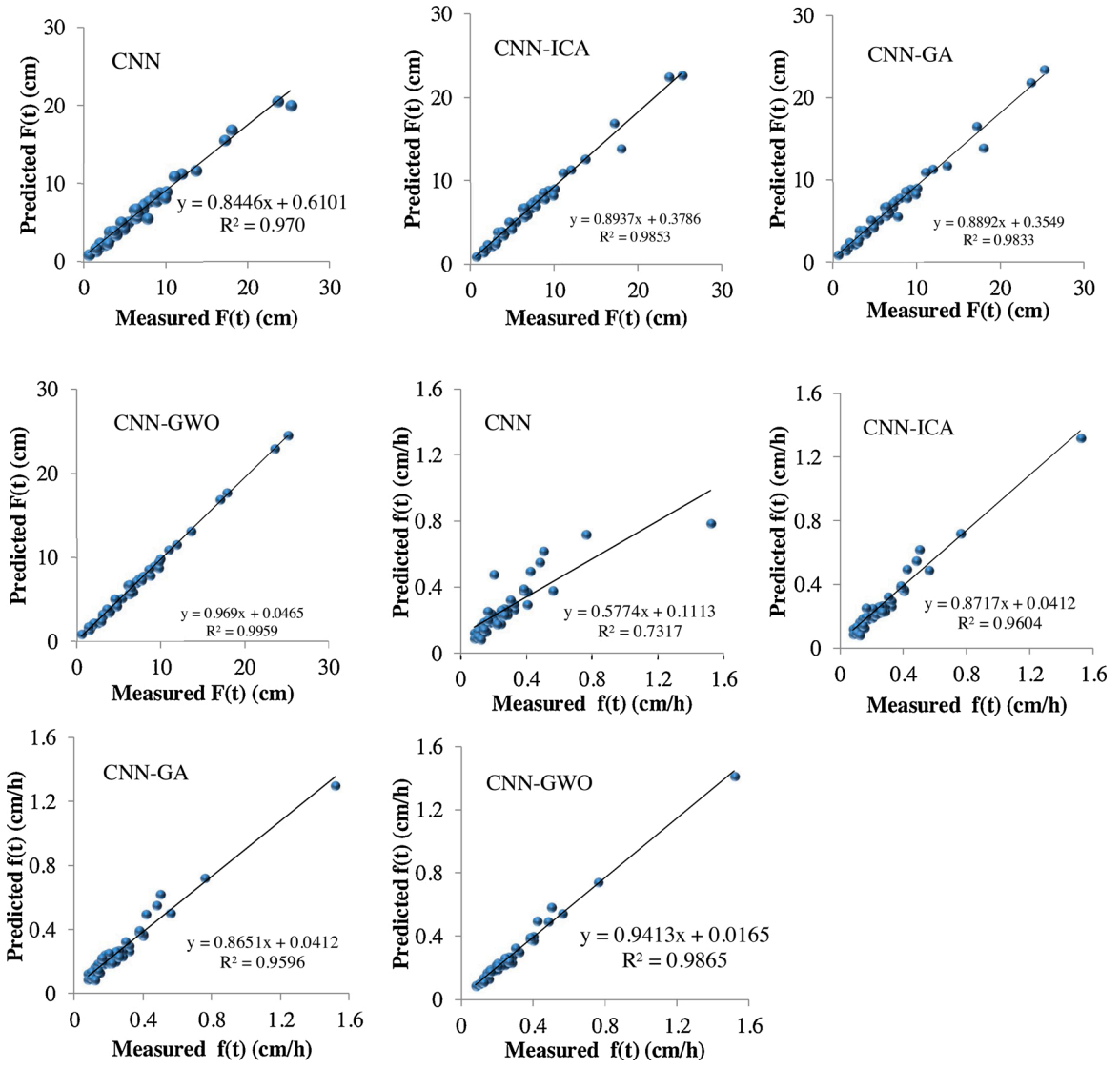

Fig. 9. Line-graph and scatter plots of predicted and measured F(t) and f(t) values during testing period.

model fits with the used training dataset. Therefore, the CNN model and its ensembles were validated by the testing datasets. Results of validation through testing data show how good and efficient the built model is for infiltration process prediction.

Fig. 9 provides line-graphs, and also a scatter plot between the measured vs. predicted values of F(t) and f(t) using CNN, CNN-ICA, CNN-GA, and CNN-GWO during the testing dataset. It is obvious that all predicted values of the models were well fitted with the measured values. Although a CNN is a powerful algorithm and has very good prediction power ($R^2 = 0.97$ and 0.73 for F(t) and f(t)), it could not predict the maximum values accurately. In general, the accuracy of any predictive model depends on several factors, e.g., the algorithm structure; the optimization of the model's parameters; the proper selection of inputs; the nature of the data; the data quality; and the size of the dataset (Asim et al., 2018). The lower prediction accuracy of CNN algorithms may be due to two main reasons: the first one is CNNs, like other neuron based models, need their parameters to be optimized; the second one is length of the data, as deep learning algorithms have a higher performance using large datasets. To enhance the prediction power of a CNN algorithm, three metaheuristic algorithms of ICA, GA, and GWO, can be coupled with a CNN to determine the model's parameter values automatically. It is obvious that optimized CNN algorithm will have a higher performance than a standalone CNN for the prediction of both F(t) and f (t), and could predict maximum values perfectly. However, F(t) predicted using the CNN-GWO model was the fittest to the measured values; it was less scattered, and demonstrated a good fit ($F(t)^{pred} = 0.969\ F(t)^{meas} + 0.046$, $R^2 = 0.995$) compared to the other models. It is followed by the CNN-ICA ($F(t)^{pred} = 0.893\ F(t)^{meas} + 0.378$, $R^2 = 0.985$), CNN-GA ($F(t)^{pred} = 0.889\ F(t)^{meas} + 0.354$, $R^2 = 0.993$), and CNN ($F(t)^{pred} = 0.742\ F(t)^{meas} + 1.097$, $R^2 = 0.969$). In the case of f(t) prediction, the line-graphs and the R^2 values indicated that the CNN-GWO was the best fit model ($f(t)^{pred} = 0.941\ f(t)^{meas} + 0.016$, $R^2 = 0.986$), followed by the CNN-ICA ($f(t)^{pred} =$

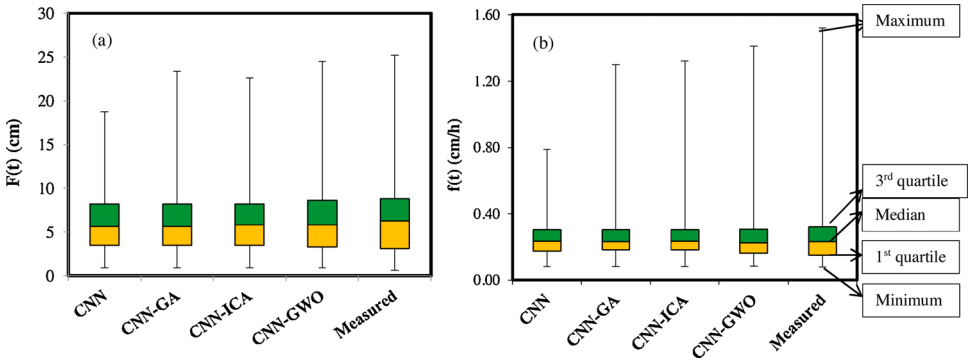

Fig. 10. Box plots of developed models : (a) F(t) and (b) f(t).

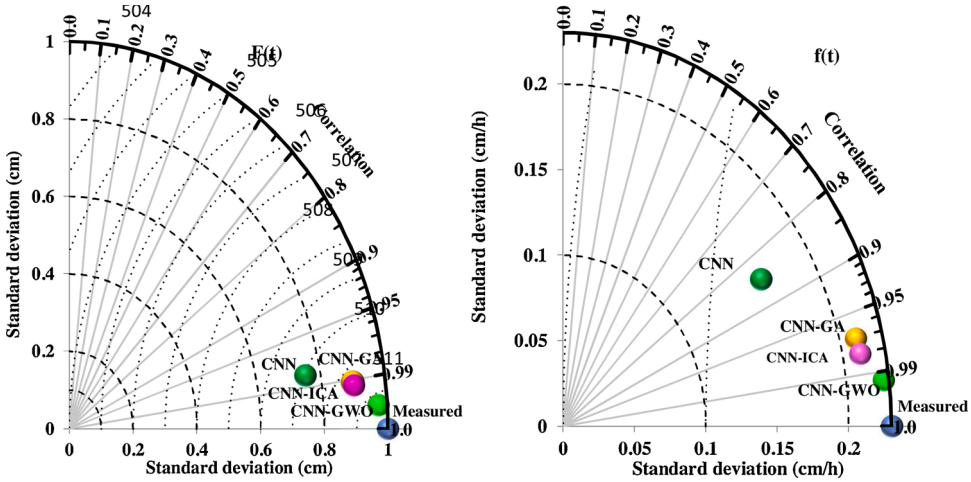

Fig. 11. Taylor plots used for evaluating performance of models: (a) F(t) and (b) f (t).

0.871 $f(t)^{meas}$ + 0.041, R^2 = 0.960), CNN-GA ($f(t)^{pred}$ = 0.865 $f(t)^{meas}$ + 0.041, R^2 = 0.959), and CNN ($f(t)^{pred}$ = 0.577 $f(t)^{meas}$ + 0.111, R^2 = 0.731). Based on the classification of goodness of fit for R^2 statistics, all three hybrid models (CNN-GWO, CNN-ICI and CNN-GA) and the standalone algorithms had 'very good' fits, for F(t) and f(t) prediction (Van Liew et al., 2003).

The box plots of the measured and predicted F(t) and f(t) using the different models were also used to assess the models' performance visually (Fig. 10). In the case of F(t), although the predicted minimum, first quartile (Q_{25}), medians (Q_{50}), and third quartile (Q_{75}) of the CNN, CNN-GA, CNN-ICA, and CNN-GWO models were closest to the measured F(t), some of the models, like CNN-GA and CNN-ICA, did not accurately predict the maximum value, and the CNN model could not satisfactorily predict the maximum F(t) value.

In the case of f(t), the results of the box plots showed that the all of the models were closest to the measure in predicting the minimum, Q_{50}, and Q_{75}, of the f(t) values, while none of them could predict the Q_{50} and maximum values accurately. In the case of maximum value, the CNN-GWO model predicted much better than the other models.

All of the models underestimated the F(t) and f(t) maximum values. The highest value is important in the prediction process because the high F(t) and f(t) values are representative of the potential contribution of infiltration to less runoff generation (less flood occurrences), and are important for groundwater recharge, soil and water conservation, and irrigation regimes in agricultural lands, and for accurate watershed management plans. Therefore, if the model predicted the maximum values inaccurately, the management plan would fail. Therefore, the best model is the one that, except for generally high accuracy, predicts the maximum value properly. Overall, the results indicated that, CNN-GWO was the fittest for the testing dataset, and it could predict maximum value well.

Taylor diagrams were plotted in order to further evaluate the models' prediction power (Fig. 11). For both F(t) and f(t) the Taylor plot indicated that the CNN-GWO model had the highest performance because the predicted standard deviation values were closely matched to those of the measured data, and the correlation coefficients were very high (0.997 and 0.985, respectively).

The visual comparison of the models' performance has the weakness that those with high performance are easily recognizable, but it is difficult to identify the models' performance classification and rank them. Thus, it is necessary to apply some quantitative measures that provide better evidence of the models' performance. Therefore, in this study, evaluation metrics were considered to compare the performance of the developed models. Fig. 12(a–d) provides the RMSE, MAE, NSE, and PBIAS values for F(t) predictions by different models. The NSE values revealed that all of the considered models had very good performance (Moriasi et al., 2007). The

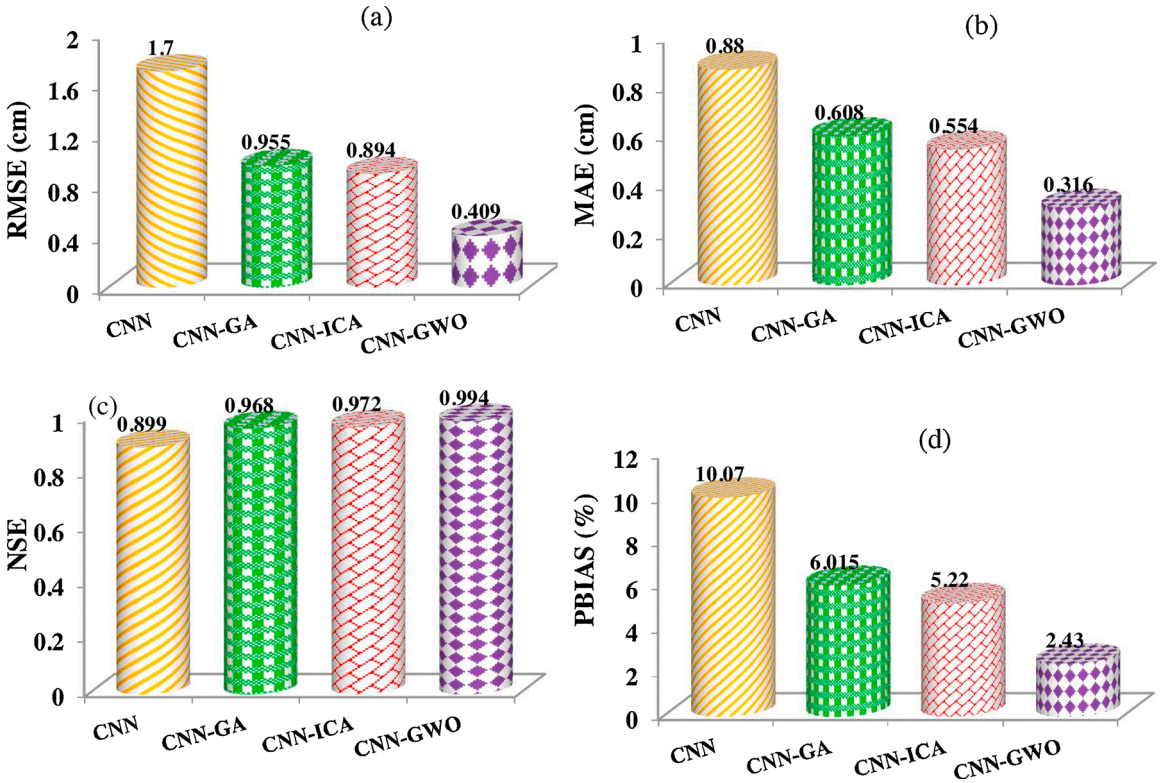

Fig. 12. Quantitative statistical metrics including RMSE (a), MAE (b), NSE (c), and PBIAS (d) in the testing phase for F(t) prediction.

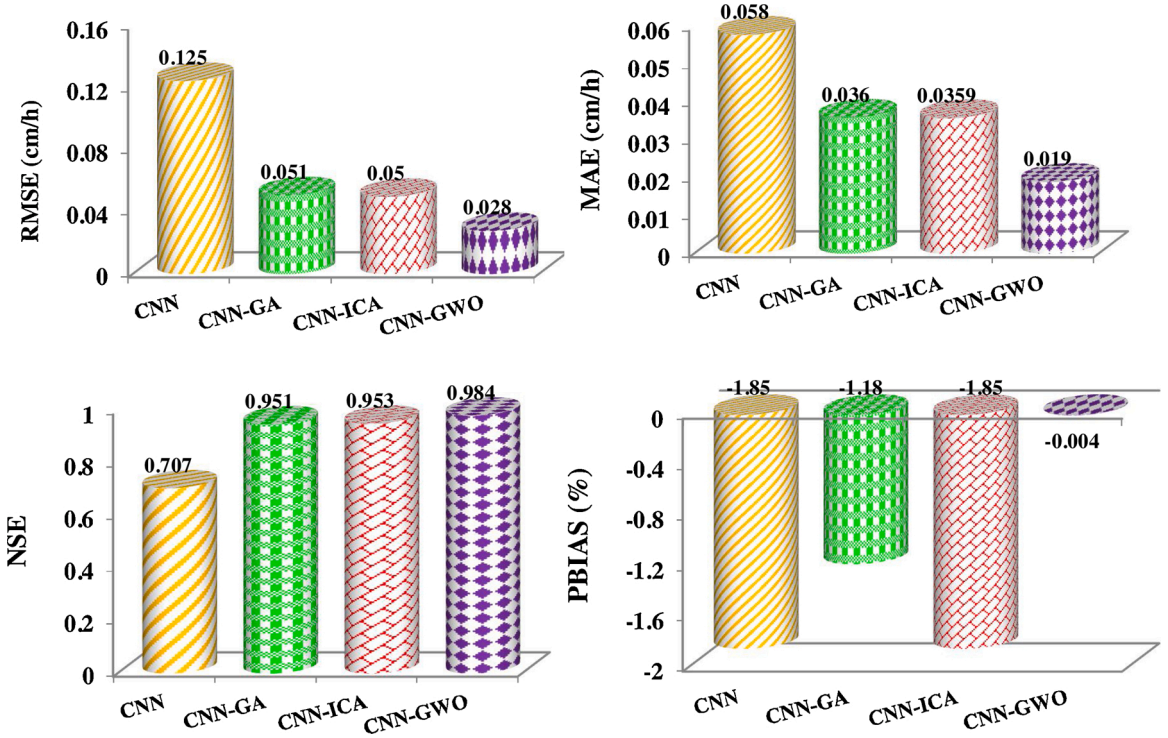

Fig. 13. Quantitative statistical metrics including RMSE (a), MAE (b), NSE, (c) and PBIAS (d) in the testing phase for f(t) prediction.

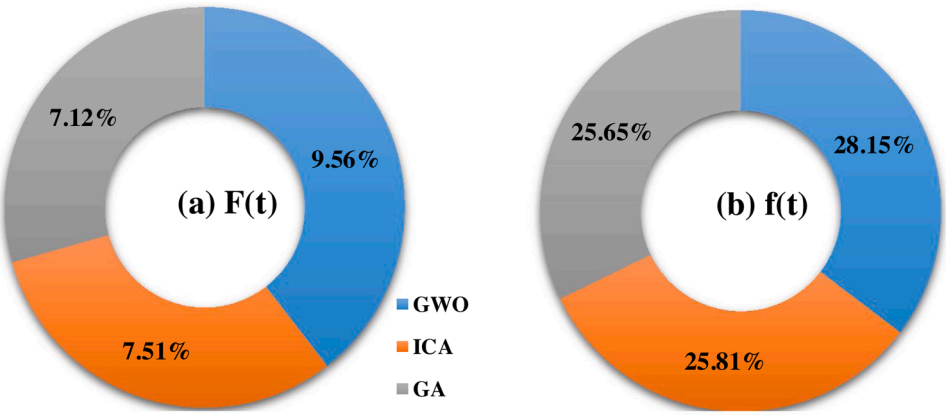

Fig. 14. Percentage of CNN improvement performance by different metaheuristic algorithms for (a) F(t) and (b) f(t).

results showed that the CNN-GWO with RMSE = 0.409 cm, MAE = 0.316 cm, NSE = 0.994, and PBIAS = 2.43 %, was the most accurate one among the optimized deep learning infiltration models, followed by the CNN-ICI, CNN-GA and CNN models. Based on the PBIAS values, all of the models underestimated the F(t) values (shown by positive PBIAS values). Moreover, the CNN-GWO, CNN-ICI, and CNN-GA model predictions were classified into very good performance (PBIAS $\leq$ 10 %), and the CNN model had good performance (10 % $\leq$ PBIAS $\leq$ 15 %).

In the case of f(t) prediction, as shown in Fig. 13, the CNN-GWO model with RMSE = 0.028 (cm/h), MAE = 0.019 (cm/h), NSE = 0.984, and PBIAS = -0.004 % outperformed the other models. It was followed by CNN-ICA, CNN-GA, and CNN models based on RMSE, MAE, and NSE measures. However, based on PBIAS criteria, CNN-GA, with a PBIAS equal to -1.18 %, outperformed the CNN-ICA (-1.85 %) and CNN (-1.85 %) models. According to NSE, optimized CNN models have a very good performance, while a standalone CNN has good prediction power. Moreover, all models overestimated f(t) values, and their performance was classified into very good performance (shown by negative PBIAS values and PBIAS $\leq$ 10 %).

Overall, based on the model performance metrics, all developed models had reasonable performance in predicting both F(t) and f(t). The present study confirmed that deep learning algorithms, here CNN, are able to model complex non-linear input-output relationships using different readily available input variables. The results of the current study showed that although a CNN algorithm is a powerful model, the hybrid models, through metaheuristic algorithms, enhanced the predictive power of the standalone CNN algorithm. The hybrid methods are considered more reasonable for environmental modeling due to more model flexibility; the determination of models' parameter values accurately; as well as the fact that they enhanced the combined effects of two standalone models (Thai Pham et al., 2019). Bui et al. (2018) stated that the hybrid models are strong and robust, and improve the power prediction of standalone models, while reducing noise and over-fitting problems (Tien Bui et al., 2018). Results of the enhanced percentage CNN algorithm by different metaheuristic algorithms are shown in Fig. 14. The results illustrated that the GWO algorithm could enhance performance of the CNN algorithm about 9.56 % and 28.18 % for F(t) and f(t) prediction, respectively. These percentages for F(t) and f(t) are 7.51 % and 25.81 for ICA algorithms and 7.12 % and 25.65 % for GA algorithms, respectively.

The main advantage of CNN algorithms compared to traditional AI algorithms are: (a) computationally efficient; (b) have many different hidden layers, which enhance prediction power; (c) automatically detect the important features without any human supervision; (d) use special convolution and pooling operations, and perform parameter sharing; and (e) use hierarchical patterns in data, and assemble more complex patterns using smaller and simpler patterns. The CNN-GWO model was known as the best performing model in the predicting of F(t) and f(t) values. The GWO was more efficient in reduction of both variance and bias, compared to the GA and ICA algorithms. The advantages of the GWO algorithm are easy to implement; less storage and fewer computational requirements; can be summarized as faster convergence, resulting from continuous reduction of search space and fewer decision variables; ability in avoiding local minima; having only two control parameters to tune the algorithm performance, and hence, better stability and robustness (Hameed et al., 2016).

Given this is the first study not only evaluating the prediction performance of optimized deep learning algorithms for F(t) and f(t) prediction, but also in geoscience, no direct comparisons exist. However, the improved performance of the hybrid models conforms to previous tests of data mining algorithms in the infiltration modeling (Arshad et al., 2013; Sihag et al., 2019b, c). There are many papers that have applied ANN algorithms to predict infiltration processes in the laboratory or with field data, and these have stated that ANN is an efficient model (Anari et al., 2011; Esmaeelnejad et al., 2015; Sedaghat et al., 2016; Sihag et al., 2018a, b). Recently, some field measurements showed the superiority of the RF model over other algorithms in infiltration rate or soil hydraulic conductivity in India (Kumar and Sihag, 2019; Sihag et al., 2019c; Singh et al., 2017). Some studies showed that SVM or GP are the models with the highest performance in infiltration characteristic prediction (Das et al., 2012; Elbisy, 2015; Sihag et al., 2018a, 2017; Sihag et al., 2018b). It is obvious from Table 1 that there is not any global agreement about which model has the highest performance, and therefore, in a new study, various models should be examined to find the best one. Thus, the performance investigation of newly developed algorithms is strongly required (like deep learning in the present study).

Additionally, some empirical, traditional AI, and data mining algorithms, with the same data of the current study were applied by

Table 5
Result of Sepahvand et al. (2018) and Sihag et al. (2018; 2019) according to R^2 metric.

No	Models	F(t)	f(t)
1	GP	0.81	–
2	SVM	**0.996**	**0.930**
3	MLR	0.35	–
4	ANFIS	0.993	0.850
5	RF	0.965	0.912
6	Kostiakov	–	0.246
7	Philips	–	0.249
8	GEP	–	0.640
9	ANN	–	0.840

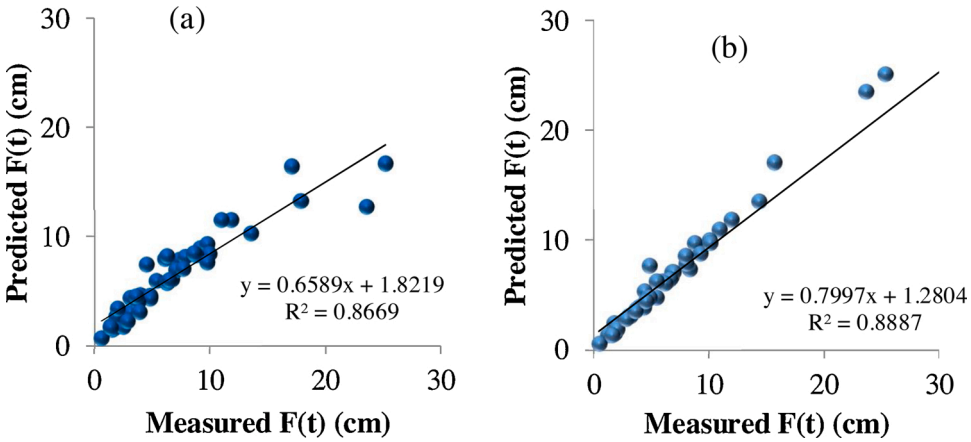

Fig. 15. Model validation and comparison: (a) SVM and (b) ANFIS algorithms.

Sepahvand et al. (2018) and Sihag et al. (2018a); Sihag et al. (2019d), whose results are tabulated in Table 5.

According to Table 4, the SVM algorithm has the same performance compared to optimized CNN-GWO algorithms, while it outperforms other algorithms for F(t) prediction. In the case of f(t) prediction, optimized CNN algorithms outperform not only SVM, but other developed algorithms. To better understand the modeling prediction power of optimized deep learning algorithms, the authors also performed SVM-RBF (Fig. 15 a) and ANFIS-trimf (Fig. 15 b), similar to what Singh et al. (2019) did, but got different prediction accuracy, which may be due to different structures of training and testing datasets. According to the new finding, the current results show that optimized CNN algorithms are more robust, flexible, and efficient algorithms, with very high prediction capability. Results demonstrate that CNN algorithms have a 11.35 % and 9.27 % higher performance than SVM and ANFIS models for F(t) prediction, respectively, while CNN-GWO was the most accurate algorithm, having has 13.65 % and 11.64 % higher performance, respectively.

As the infiltration process not only changes spatially, but also temporally, it is recommended to collect various time series data and investigate the prediction power of AI models to predict the infiltration process. Cerdà (1997) reported that seasonal changes play important roles in soil hydrology, whereas the infiltration rate was the highest during the summer each year (Fang et al., 1958).

5. Conclusion

The present study evaluated the effectiveness of the stand-alone and optimized deep learning of convolutional neural network (CNN) algorithms, using three metaheuristic algorithms for cumulative infiltration and infiltration rate prediction in Iran. The main results of the current study are summarized as follows:

1 All developed algorithms have very good performance for both cumulative infiltration and infiltration rate prediction.
2 A CNN model optimized with a GWO algorithm outperformed the other algorithms, followed by CNN-ICA, CNN-GA, and a stand-alone CNN algorithm.
3 Metaheuristic algorithms enhanced the prediction capability of a stand-alone CNN algorithm significantly, about 9.56 %, 7.51 %, and 7.21 % for cumulative infiltration, and about 28.15 %, 25.81 % and 25.65 % for infiltration rate prediction for GWO, ICA, and GA algorithms, respectively.
4 Different input variables lead to different prediction performance.
5 Time of experiment measurement has the highest effect on the cumulative infiltration, followed by % of silt, % of clay, % of sand, moisture content, soil density, and infiltration rate, respectively.

6 Percentage of silt is the most important parameter on infiltration rate prediction, followed by time, % of clay, moisture content, % of sand, and soil density.
7 All developed algorithms underestimated cumulative infiltration, while overestimating infiltration rates.
8 Not only optimized CNN algorithms, but also a stand-alone CNN algorithm outperformed over all traditional machine learning (GP, RF, GEP, ANN, SVR, SVM, and ANFIS) and empirical models (Kostiakov and Philips).

The present results show that stand-alone and optimized CNN algorithms are cost-effective tools, which are not only proposed to be used in infiltration process in other parts of the world, but also in all aspects of hydrological science, especially phenomena with complicated processes.

Contribution

Mahdi Panahi: Software, conceptualization; Khabat Khosravi: Conceptualization, Methodology, Writing – original draft, review and editing; Sajad Ahmad; Conceptualization, Review and editing; Somaye Panahi: Writing – original draft; Salim Heddam: Writing – original draft; Assefa Melesse: review and editing; Ebrahim Omidvar; Writing – original draft; Chang-Wook Lee: review and editing and supervisor.

Declaration of Competing Interest

The authors report no declarations of interest.

Acknowledgements

This research was supported by a grant from the National Research Foundation of Korea provided by the government of Korea (No. 2019R1A2C1085686). Also, we would like to thank the Editor-in-chief **Prof. Patrick Willems** and two anonymous reviewers for their very useful feedback on the initial manuscript, which helped to significantly improve the quality of this paper.

Appendix A. Supplementary data

Supplementary material related to this article can be found, in the online version, at doi:https://doi.org/10.1016/j.ejrh.2021.100825.

References

Ahmad, S., Simonovic, S.P., 2005. An artificial neural network model for generating hydrograph from hydro-meteorological parameters. J. Hydrol. 315 (1–4), 236–251.
Ahmad, S., Kalra, A., Stephen, H., 2010. Estimating soil moisture using remote sensing data: a machine learning approach. Adv. Water Resour. 33 (1), 69–80.
Ahmad, M.W., Reynolds, J., Rezgui, Y., 2018. Predictive modelling for solar thermal energy systems: a comparison of support vector regression, random forest, extra trees and regression trees. J. Clean. Prod. 203, 810–821.
Anari, P.L., Darani, H.S., Nafarzadegan, A., 2011. Application of ANN and ANFIS models for estimating total infiltration rate in an arid rangeland ecosystem. Res. J. Environ. Sci. 5 (3), 236–247.
Angelaki, A., Sakellariou-Makrantonaki, M., Tzimopoulos, C., 2004. Laboratory experiments and estimation of cumulative infiltration and sorptivity. Water Air Soil Pollut. Focus. 4 (4–5), 241–251.
Angelaki, A., Sakellariou-Makrantonaki, M., Tzimopoulos, C., 2013. Theoretical and experimental research of cumulative infiltration. Transp. Porous Media 100 (2), 247–257.
Angelaki, A., Singh Nain, S., Singh, V., Sihag, P., 2018. Estimation of models for cumulative infiltration of soil using machine learning methods. ISH J. Hydraul. Eng. 1–8.
Arshad, R.R., Sayyad, G., Mosaddeghi, M., Gharabaghi, B., 2013. Predicting saturated hydraulic conductivity by artificial intelligence and regression models. ISRN Soil Sci. 2013.
Asim, Y., Shahid, A.R., Malik, A.K., Raza, B., 2018. Significance of machine learning algorithms in professional blogger's classification. Comput. Electr. Eng. 65, 461–473.
Atashpaz-Gargari, E., Lucas, C., 2007. Imperialist competitive algorithm: an algorithm for optimization inspired by imperialistic competition. In: 2007 IEEE Congress on Evolutionary Computation. IEEE, pp. 4661–4667.
Ateeq-ur-Rauf, Ghumman, A.R., Ahmad, S., Hashmi, H.N., 2018. Performance assessment of artificial neural networks and support vector regression models for stream flow predictions. Environ. Monit. Assess. https://doi.org/10.1007/s10661-018-7012-9.
Ayele, G.T., Teshale, E.Z., Yu, B., Rutherfurd, I.D., Jeong, J., 2017. Streamflow and sediment yield prediction for watershed prioritization in the Upper Blue Nile River Basin, Ethiopia. Water 9 (10), 782.
Barkhoda, W., Sheikhi, H., 2020. Immigrant imperialist competitive algorithm to solve the multi-constraint node placement problem in target-based wireless sensor networks. Ad Hoc Netw. 106, 102183.
Behrahi, K., Sayyad, G., Landi, A., peyrowan, H., 2018. Effect of landuse type and land slope degree on runoff quantity using artificial rain simulaitor, case study: Kakasharaf watershed. Watershed Eng. Manage. J. 10 (1), 58–70.
Bui, D.T., et al., 2020a. A novel deep learning neural network approach for predicting flash flood susceptibility: a case study at a high frequency tropical storm area. Sci. Total Environ. 701, 134413.
Bui, D.T., Tsangaratos, P., Nguyen, V.-T., Van Liem, N., Trinh, P.T., 2020b. Comparing the prediction performance of a Deep Learning Neural Network model with conventional machine learning models in landslide susceptibility assessment. CATENA 188, 104426.
Cerdà, A., 1997. Seasonal changes of the infiltration rates in a Mediterranean scrubland on limestone. J. Hydrol. 198 (1–4), 209–225.

Cheik, S., Bottinelli, N., Sukumar, R., Jouquet, P., 2018. Fungus-growing termite foraging activity increases water infiltration but only slightly and temporally impacts soil physical properties in southern Indian woodlands. Eur. J. Soil Biol. 89, 20–24.
Choubin, B., Khalighi-Sigaroodi, S., Malekian, A., Ahmad, S., Attarod, P., 2014. Drought forecasting in a semi-arid watershed using climate signals: a neuro-fuzzy modeling approach. J. Sci. 11 (6), 1593–1605.
Das, S.K., Samui, P., Sabat, A.K., 2012. Prediction of field hydraulic conductivity of clay liners using an artificial neural network and support vector machine. Int. J. Geomech. 12 (5), 606–611.
Dehghani, M., Seifi, A., Riahi-Madvar, H., 2019. Novel forecasting models for immediate-short-term to long-term influent flow prediction by combining ANFIS and grey wolf optimization. J. Hydrol. 576, 698–725.
Dehghani, M., Mashayekhi, M., Sharifi, M., 2021. An efficient imperialist competitive algorithm with likelihood assimilation for topology, shape and sizing optimization of truss structures. Appl. Math. Model. 93, 1–27.
Demand, D., Selker, J.S., Weiler, M., 2019. Influences of macropores on infiltration into seasonally frozen soil. Vadose Zone J. 18 (1).
Di Persio, L., Honchar, O., 2016. Artificial neural networks architectures for stock price prediction: comparisons and applications. Int. J. Circuits, Syst. Sig. Process. 10, 403–413.
Ding, C., 2020. Convolutional neural networks for particle shape classification using light-scattering patterns. J. Quant. Spectrosc. Radiat. Transf. 245, 106901.
Elbisy, M.S., 2015. Support vector machine and regression analysis to predict the field hydraulic conductivity of sandy soil. KSCE J. Civ. Eng. 19 (7), 2307–2316.
Esmaeelnejad, L., Ramezanpour, H., Seyedmohammadi, J., Shabanpour, M., 2015. Selection of a suitable model for the prediction of soil water content in north of Iran. Span. J. Agric. Res. 13 (1), 1202.
Fan, Y., Huang, N., Gong, J., Shao, X., Zhang, J., 2018. A simplified infiltration model for predicting cumulative infiltration during vertical line source irrigation. Water 10 (1), 89.
Fan, D., Wang, S., Guo, Y., Zhu, Y., Agathokleous, E., Ahmad, S., Han, J., 2020a. Cd induced biphasic response in soil alkaline phosphatase and changed soil bacterial community composition: the role of background Cd contamination and time as additional factors. Sci. Total Environ. https://doi.org/10.1016/j.scitotenv.2020.143771.
Fan, D., Jing, J., Zhu, Y., Ahmad, S., Han, J., 2020b. Toluene induces hormetic response of soil alkaline phosphatase and the potential enzyme kinetic mechanism. Ecotoxicol. Environ. Saf. 206, 111123 https://doi.org/10.1016/j.ecoenv.2020.111123.
Fang, Z., Yang, W., Zhou, P., 1958. Investigation Research on Loess Plateau Terrace in Middle Reaches of Yellow River. Science Press, Beijing, China.
Fukushima, K., 1988. Neocognitron: a hierarchical neural network capable of visual pattern recognition. Neural Netw. 1 (2), 119–130.
Ghumman, A.R., Iqbal, M., Ahmad, S., Hashmi, H.N., 2018a. Experimental and numerical investigations for optimal emitter spacing in drip irrigation. Irrig. Drain. 67, 724–737. https://doi.org/10.1002/ird.2284.
Ghumman, A.R., Ahmad, S., Rahman, S., Khan, Z., 2018b. Investigating management of irrigation water in the upstream control system of the Upper Swat Canal. Iran. J. Sci. Technol. Trans. Civil Eng. https://doi.org/10.1007/s40996-018-0097-0.
Goodfellow, I., Bengio, Y., Courville, A., 2016. Deep Learning. MIT press.
Green, W., Ampt, G., 1911. The flow of air and water through soils. J. Agric. Sci. 4, 1–24.
Gunduz, H., Yaslan, Y., Cataltepe, Z., 2017. Intraday prediction of Borsa Istanbul using convolutional neural networks and feature correlations. Knowl. Based Syst. 137, 138–148.
Hameed, I.A., Bye, R.T., Osen, O.L., 2016. Grey wolf optimizer (GWO) for automated offshore crane design. In: 2016 IEEE Symposium Series on Computational Intelligence (SSCI). IEEE, pp. 1–6.
Hooshyar, M., Wang, D., 2016. An analytical solution of Richards' equation providing the physical basis of SCS curve number method and its proportionality relationship. Water Resour. Res. 52 (8), 6611–6620.
Horton, R.E., 1941. An approach toward a physical interpretation of infiltration-capacity 1. Soil Sci. Soc. Am. J. 5 (C), 399–417.
Hoseinzade, E., Haratizadeh, S., 2019. CNNpred: CNN-based stock market prediction using a diverse set of variables. Expert Syst. Appl. 129, 273–285.
Hu, P., Pan, J.-S., Chu, S.-C., 2020. Improved binary Grey Wolf Optimizer and its application for feature selection. Knowl. Based Syst., 105746
Huang, J., Monteiro Santos, F., Triantafilis, J., 2016. Mapping soil water dynamics and a moving wetting front by spatiotemporal inversion of electromagnetic induction data. Water Resour. Res. 52 (11), 9131–9145.
Indolia, S., Goswami, A.K., Mishra, S., Asopa, P., 2018. Conceptual understanding of convolutional neural network-a deep learning approach. Procedia Comput. Sci. 132, 679–688.
Iyer, V.H., Mahesh, S., Malpani, R., Sapre, M., Kulkarni, A.J., 2019. Adaptive range genetic algorithm: a hybrid optimization approach and its application in the design and economic optimization of shell-and-tube heat exchanger. Eng. Appl. Artif. Intell. 85, 444–461.
Jejurkar, C.L., Rajurkar, M.P., 2015. An investigational approach for the modelling of infiltration process in a clay soil. KSCE J. Civ. Eng. 19 (6), 1916–1921.
Kakandikar, G.M., Nandedkar, V.M., 2016. Prediction and optimization of thinning in automotive sealing cover using genetic algorithm. J. Comput. Des. Eng. 3 (1), 63–70.
Kale, R.V., Sahoo, B., 2011. Green-Ampt infiltration models for varied field conditions: a revisit. Water Resour. Manag. 25 (14), 3505.
Karasu, S., Saraç, Z., 2020. Classification of power quality disturbances by 2D-Riesz Transform, multi-objective grey wolf optimizer and machine learning methods. Digit. Signal Process., 102711
Khatri, K., Smith, R., 2006. A real time control system for furrow irrigation to manage spatial and temporal variations infiltration. Irrig. Sci 25, 33–43.
Kisi, O., Dailr, A.H., Cimen, M., Shiri, J., 2012. Suspended sediment modeling using genetic programming and soft computing techniques. J. Hydrol. 450, 48–58.
Kofinas, P., Dounis, A., Vouros, G., 2018. Fuzzy Q-learning for multi-agent decentralized energy management in microgrids. Appl. Energy 219, 53–67.
Kostiakov, A.N., 1932. On the dynamics of the coefficient of water percolation in soils and the necessity of studying it from the dynamic point of view for the purposes of amelioration. Trans. Sixth Comm. Int. Soc. Soil Sci. 1, 7–21.
Krause, P., Boyle, D., Bäse, F., 2005. Comparison of different efficiency criteria for hydrological model assessment. Adv. Geosci. 5, 89–97.
Kujawa, S., Mazurkiewicz, J., Czekała, W., 2020. Using convolutional neural networks to classify the maturity of compost based on sewage sludge and rapeseed straw. J. Clean. Prod., 120814
Kumar, M., Sihag, P., 2019. Assessment of Infiltration rate of soil using empirical and machine learning-based models. Irrig. Drain. 68 (3), 588–601.
Lassabatere, L., Angulo-Jaramillo, R., Soria-Ugalde, J., Šimůnek, J., Haverkamp, R., 2009. Numerical evaluation of a set of analytical infiltration equations. Water Resour. Res. 45 (12).
LeCun, Y., Bengio, Y., 1995. Convolutional networks for images, speech, and time series. In: The Handbook of Brain Theory and Neural Networks, 3361 (10): 1995.
Legates, D.R., McCabe Jr., G.J., 1999. Evaluating the use of "goodness-of-fit" measures in hydrologic and hydroclimatic model validation. Water Resour. Res. 35 (1), 233–241.
Li, K., Zhou, G., Yang, Y., Li, F., Jiao, Z., 2020. A novel prediction method for favorable reservoir of oil field based on grey wolf optimizer and twin support vector machine. J. Pet. Sci. Eng., 106952
Luo, K., Zhao, Q., 2019. A binary grey wolf optimizer for the multidimensional knapsack problem. Appl. Soft Comput. 83, 105645.
Ma, J., Li, L.H., Guo, L.P., Bai, L., Zhang, J.R., Chen, Z.H., Ahmad, S., 2015. Variation in soil nutrients in grasslands along the Kunes River in Xinjiang, China. Chem. Ecol. 31 (2), 111–122.
Mahapatra, S., Jha, M.K., Biswal, S., Senapati, D., 2020. Assessing variability of infiltration characteristics and reliability of infiltration models in a tropical sub-humid region of india. Sci. Rep. 10 (1), 1–18.
Mahmood, S., Latif, M., 2003. Surge-ring infiltrometer and its application to simulate infiltration. Irrig. Drain. Syst. 17 (4), 367–379.
Maiti, A., Maiti, M., 2008. Discounted multi-item inventory model via genetic algorithm with Roulette wheel selection, arithmetic crossover and uniform mutation in constraints bounded domains. Int. J. Comput. Math. 85 (9), 1341–1353.
Melesse, A., Ahmad, S., McClain, M., Wang, X., Lim, Y., 2011. Suspended sediment load prediction of river systems: an artificial neural network approach. Agric. Water Manag. 98 (5), 855–866.

Mirjalili, S., Mirjalili, S.M., Lewis, A., 2014. Grey wolf optimizer. Adv. Eng. Softw. 69, 46–61.
Montazeri-Gh, M., Poursamad, A., Ghalichi, B., 2006. Application of genetic algorithm for optimization of control strategy in parallel hybrid electric vehicles. J. Franklin Inst. 343 (4–5), 420–435.
Moriasi, D.N., et al., 2007. Model evaluation guidelines for systematic quantification of accuracy in watershed simulations. Trans. ASABE 50 (3), 885–900.
Pahlavan-Rad, M.R., et al., 2020. Prediction of soil water infiltration using multiple linear regression and random forest in a dry flood plain, eastern Iran. Catena 194, 104715.
Pham, B.T., Bui, D.T., Prakash, I., Dholakia, M., 2017. Hybrid integration of multilayer perceptron neural networks and machine learning ensembles for landslide susceptibility assessment at himalayan area (India) using GIS. Catena 149, 52–63.
Philip, J., 1957a. The theory of infiltration: 1. The infiltration equation and its solution. Soil Sci. 83 (5), 345–358.
Philip, J.R., 1957b. The theory of infiltration: 4. Sorptivity and algebraic infiltration equations. Soil Sci. 84 (3), 257–264.
Puri, S., Stephen, H., Ahmad, S., 2011. Relating TRMM precipitation radar land surface backscatter response to soil moisture in the Southern United States. J. Hydrol. 402 (1–2), 115–125.
Rahmati, M., 2017. Reliable and accurate point-based prediction of cumulative infiltration using soil readily available characteristics: a comparison between GMDH, ANN, and MLR. J. Hydrol. 551, 81–91.
Rashid, T.A., Abbas, D.K., Turel, Y.K., 2019. A multi hidden recurrent neural network with a modified grey wolf optimizer. PLoS One 14 (3).
Reisi, N., Lakmesari, S.H., Mahmoodabadi, M., Hadipour, S., 2019. Optimum fuzzy control of human immunodeficiency virus type1 using an imperialist competitive algorithm. Inform. Med. Unlocked 16, 100241.
Richards, L.A., 1931. Capillary conduction of liquids through porous mediums. Physics 1 (5), 318–333.
Roshanaei, M., Lucas, C., Mehrabian, A., 2009. Adaptive beamforming using a novel numerical optimisation algorithm. IET Microw. Antennas Propag. 3 (5), 765–773.
Rozinajová, V., et al., 2018. Computational intelligence in smart grid environment. Computational Intelligence for Multimedia Big Data on the Cloud with Engineering Applications. Elsevier, pp. 23–59.
Samadianfard, S., Ghorbani, M.A., Mohammadi, B., 2018. Forecasting soil temperature at multiple-depth with a hybrid artificial neural network model coupled-hybrid firefly optimizer algorithm. Inf. Process. Agric. 5 (4), 465–476.
Samadianfard, S., Jarhan, S., Salwana, E., Mosavi, A., Shamshirband, S., Akib, S., 2019. Support vector regression integrated with fruit fly optimization algorithm for river flow forecasting in Lake Urmia Basin. Water 11 (9), 1934.
Saxena, A., Kumar, R., Mirjalili, S., 2020. A harmonic estimator design with evolutionary operators equipped grey wolf optimizer. Expert Syst. Appl. 145, 113125.
SCS, U., 1972. National Engineering Handbook. Hydrology Section, 4.
Sedaghat, A., Bayat, H., Sinegani, A.S., 2016. Estimation of soil saturated hydraulic conductivity by artificial neural networks ensemble in smectitic soils. Eurasian Soil Sci. 49 (3), 347–357.
Sepahvand, A.S., Sihag, P., Singh, B., Zand, M., 2018. Comparative evaluation of infiltration models. KSCE J. Civ. Eng. 22 (10), 4173–4184.
Sigaroodi, S.K., Chen, Q., Ebrahimi, S., Nazari, A., Choobin, B., 2014. Long-term precipitation forecast for drought relief using atmospheric circulation factors: a study on the Maharloo Basin in Iran. Hydrol. Earth Syst. Sci. 18 (5), 1995.
Sihag, P., Tiwari, N., Ranjan, S., 2017. Modelling of infiltration of sandy soil using gaussian process regression. Model. Earth Syst. Environ. 3 (3), 1091–1100.
Sihag, P., Jain, P., Kumar, M., 2018a. Modelling of impact of water quality on recharging rate of storm water filter system using various kernel function based regression. Model. Earth Syst. Environ. 4 (1), 61–68.
Sihag, P., Tiwari, N., Ranjan, S., 2018b. Support vector regression-based modeling of cumulative infiltration of sandy soil. ISH J. Hydraul Eng.
Sihag, P., Karimi, S.M., Angelaki, A., 2019a. Random forest, M5P and regression analysis to estimate the field unsaturated hydraulic conductivity. Appl. Water Sci. 9 (5), 129.
Sihag, P., et al., 2019b. Modelling of infiltration using artificial intelligence techniques in semi-arid Iran. Hydrol. Sci. J. 64 (13), 1647–1658.
Sihag, P., Tiwari, N., Ranjan, S., 2019c. Prediction of cumulative infiltration of sandy soil using random forest approach. J. Appl. Water Eng. Res. 7 (2), 118–142.
Sihag, P., Tiwari, N., Ranjan, S., 2019d. Prediction of unsaturated hydraulic conductivity using adaptive neuro-fuzzy inference system (ANFIS). ISH J. Hydraul. Eng. 25 (2), 132–142.
Sihag, P., Kumar, M., Singh, B., 2020a. Assessment of infiltration models developed using soft computing techniques. Geol. Ecol. Landsc. 1–11.
Sihag, P., Singh, B., Sepah Vand, A., Mehdipour, V., 2020b. Modeling the infiltration process with soft computing techniques. ISH J. Hydraul. Eng. 26 (2), 138–152.
Sihag, P., Tiwari, N., Ranjan, S., 2020c. Support vector regression-based modeling of cumulative infiltration of sandy soil. ISH J. Hydraul. Eng. 26 (1), 44–50.
Singh, B., Sihag, P., Singh, K., 2017. Modelling of impact of water quality on infiltration rate of soil by random forest regression. Model. Earth Syst. Environ. 3 (3), 999–1004.
Singh, B., Sihag, P., Deswal, S., 2019a. Modelling of the impact of water quality on the infiltration rate of the soil. Appl. Water Sci. 9 (1), 15.
Singh, B., Sihag, P., Pandhiani, S.M., Debnath, S., Gautam, S., 2019b. Estimation of permeability of soil using easy measured soil parameters: assessing the artificial intelligence-based models. ISH J. Hydraul. Eng. 1–11.
Sivanandam, S., Deepa, S., 2008. Genetic Algorithms, Introduction to Genetic Algorithms. Springer, pp. 15–37.
Stephen, H., Ahmad, S., Piechota, T.C., Tang, C., 2010. Relating surface backscatter response from TRMM precipitation radar to soil moisture: results over a semi-arid region. Hydrol. Earth Syst. Sci. 14 (2), 193–204.
Sy, N.L., 2006. Modelling the infiltration process with a multi-layer perceptron artificial neural network. Hydrol. Sci. J. 51 (1), 3–20.
Thai Pham, B., et al., 2019. Landslide susceptibility assessment by novel hybrid machine learning algorithms. Sustainability 11 (16), 4386.
Thakur, B., Kalra, A., Ahmad, S., Lamb, K., Lakshmi, V., 2020. bringing statistical learning machines together for hydro-climatological predictions – case study for Sacramento San Joaquin River Basin, California. J. Hydrol. Reg. Stud. https://doi.org/10.1016/j.ejrh.2019.100651.
Tien Bui, D., et al., 2018. New hybrids of anfis with several optimization algorithms for flood susceptibility modeling. Water 10 (9), 1210.
Van Liew, M., Arnold, J., Garbrecht, J., 2003. Hydrologic simulation on agricultural watersheds: choosing between two models. Trans. ASAE 46 (6), 1539.
Wang, Y., Fang, Z., Wang, M., Peng, L., Hong, H., 2020. Comparative study of landslide susceptibility mapping with different recurrent neural networks. Comput. Geosci. 138, 104445.
Wu, L., et al., 2019. A deep learning model to recognize food contaminating beetle species based on elytra fragments. Comput. Electron. Agric. 166, 105002.
Yang, M.-D., Yang, Y.-F., Su, T.-C., Huang, K.-S., 2014. An efficient fitness function in genetic algorithm classifier for landuse recognition on satellite images. Sci. World J. 2014.
Yang, B., Zhang, X., Yu, T., Shu, H., Fang, Z., 2017. Grouped grey wolf optimizer for maximum power point tracking of doubly-fed induction generator based wind turbine. Energy Convers. Manage. 133, 427–443.
Yaseen, Z.M., El-Shafie, A., Jaafar, O., Afan, H.A., Sayl, K.N., 2015. Artificial intelligence based models for stream-flow forecasting: 2000–2015. J. Hydrol. 530, 829–844.
Yilmaz, I., Marschalko, M., Bednarik, M., Kaynar, O., Fojtova, L., 2012. Neural computing models for prediction of permeability coefficient of coarse-grained soils. Neural Comput. Appl. 21 (5), 957–968.
Zaller, J.G., Heigl, F., Ruess, L., Grabmaier, A., 2014. Glyphosate herbicide affects belowground interactions between earthworms and symbiotic mycorrhizal fungi in a model ecosystem. Sci. Rep. 4, 5634.
Zhu, X., Cai, Z., Wu, J., Cheng, Y., Huang, Q., 2019. Convolutional neural network based combustion mode classification for condition monitoring in the supersonic combustor. Acta Astronaut. 159, 349–357.
Zolfaghari, A., Mirzaee, S., Gorji, M., 2012. Comparison of different models for estimating cumulative infiltration. Int. J. Soil Sci. 7 (3), 108.